Imaging of Highly Dipping Strata and Growth Fault in Vainateyam Area, KG Basin Using Insitu Angle Domain Techniques

V P Singh, Saheb Ghosh, K S Negi*
Oil and Natural Gas Corporation Limited

singh_vp1@ongc.co.in

Keywords

Full Azimuth reflection grid tomography, Local Angle Domain Imaging, Specular and Diffraction Imaging

Summary

The study area, Vinateyam, KG Basin, is both structurally and stratigraphically complex due to presence of high-dips, rapid lateral structural variation and complex growth faulting. So imaging of high dips, delineation of fault networks and enhancing the continuity of deeper sequences are prime imaging objectives. In this work full azimuth reflection grid tomography is preformed to build a depth interval velocity model that can properly encounter structural variations. Local angle domain wavefield separation, specular and diffraction imaging is then performed. The specular stack imaged highly dipping reflectors and shows enhance continuity of deep-seated structures. Diffraction stack clearly brought out major-minor faults and the steep dip events. Combination of specular and diffraction stack gives good confidence on growth fault delineation. Significant improvements are seen in terms of reflector continuity, fault delineation, and imaging of deeper reflector.

Introduction

The area under study, Vainateyam of Krishna-Godavari Basin, lies on the east coast of India. The area comprised of both transition zone and shallow water (figure.1), seismic data was acquired using Ocean Bottom Cable (OBC) technique. Different geometries were used for land and water part. Full fold data volume is 652 SKM comprising of 55 SKM onland data and 597 SKM offshore data with a bin size of 12.5mx25m. This paper describe the processes and outputs of isotropic prestack depth domain imaging. So the depth domain processing starts from offset regularized CMP gather at MSL.

The area is structurally complex due to marine transgressive motion, high bed dips, rotation of strata and growth fault tectonics. So proper structural mapping and precise delineation of subsurface discontinuity is necessary for hydrocarbon prospect identification and reserve estimation in this area. Now success of seismic imaging demands a depth-interval velocity model that can encounter rapid lateral variation and a good migration algorithm which is able to image steep dips. Here Full azimuth reflection grid tomography is used to build the depth-interval velocity model. In-situ local angle domain (LAD) imaging (Koren, 2011) is then performed. LAD imaging takes care for ray bending, multi arrivals and true amplitude preservation. Also it decompose migrated energy in reflection and diffraction, hence an improvement in reflector continuity in the specular stack and delineation of structural discontinuities in diffraction stack. The combine stacks gives improved subsurface insights.

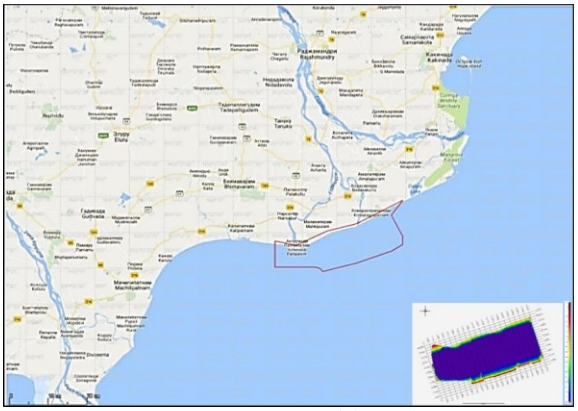

Figure.1 Location map of the study area

Geology of the Study Area

Krishna-Godavari basin was a major intra-cratonic basin within the greater Gondwanaland landmass during Late Carboniferous, Permian and Triassic (NW-SE trending Pranhita Godavari basin).

The break-up of Gondwanaland during Late Jurassic-Early Cretaceous resulted in the development of a syn-rift basin that is represented today by the NE-SW trending horst and graben features. The Matsyapuri-Palakollu fault is the major onland fault. Since Late Cretaceous, the basin became a passive margin basin. There was large-scale marine transgression in the Paleocene represented by Palakollu Shale. The rapid depositions of huge sediments from the shelf area together with syndepositional growth fault tectonics are responsible for gradual increase of Eocene sedimentary thickness towards the basin. The Eocene deltaic sands (Pasarlapudi play) are major hydrocarbon bearing reservoirs, immediately south of Matsyapuri-Palakolu fault system. The fields like Pasarlapudi, Tatipaka, Razole, Lakshmaneswaram, Elamanchili, Rangapuram and East Rangapuram are producers from these reservoirs.

Miocene top is marked by an erosional unconformity of Early Pliocene age. The sediments of Miocene and older ages eroded during this unconformity have probably been redeposit as the ubiquitous Mass Transport Complex (MTC) in deep-water area. It is overlain by Godavari clay of Pliocene-Recent age; a number of channel sand layers are encountered within it. Main imaging objective is better structural mapping of Eocene/Miocene (1500m – 4500m in depth) sands, confirmation of major-minor faults and imaging of deeper structure to understand the basin configuration.

Methodology

A depth interval velocity model represents underneath geological structures. So, estimation of a geologically reliable depth interval velocity from reflection data is one of the major task in depth-imaging. This velocity with a good migration algorithm then places the surface recorded energy at an accurate 3D subsurface location. Figure.2 describes the details workflow. The major steps are:

- Estimation of initial depth-interval velocity model.
- Upgradation of depth-interval velocity using full azimuth reflection grid tomography
- Local angle domain wavefield separation, specular and diffraction imaging.

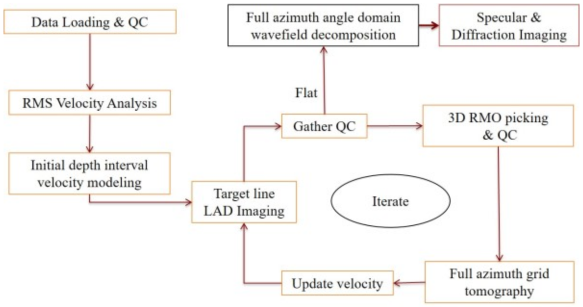

Figure.2 Depth imaging workflow

At first RMS velocity analysis is performed on target line Kirchhoff's Pre-Stack Time Migration (PSTM) gathers. This RMS velocity is then further refined by doing residual analysis on the migrated PSTM gather. Initial depth interval velocity model is then built from this final RMS velocity using Constrained Dix Inversion (Koren, 2006). Constrained dix inversion produce stable depth interval velocity in comparison to mathematical dix inversion. During inversion it utilizes different weightage on data misfit, trend and damping to give confidence on RMS picks and to stabilize the inversion.

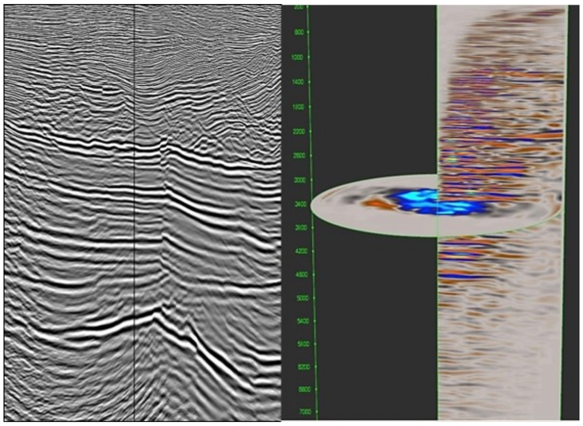

Figure.3 3D reflection angle-azimuth gather

Local angle domain target line imaging is then performed. Residual move outs are autopicked on 3D reflection angle-azimuth gathers (figure.3).

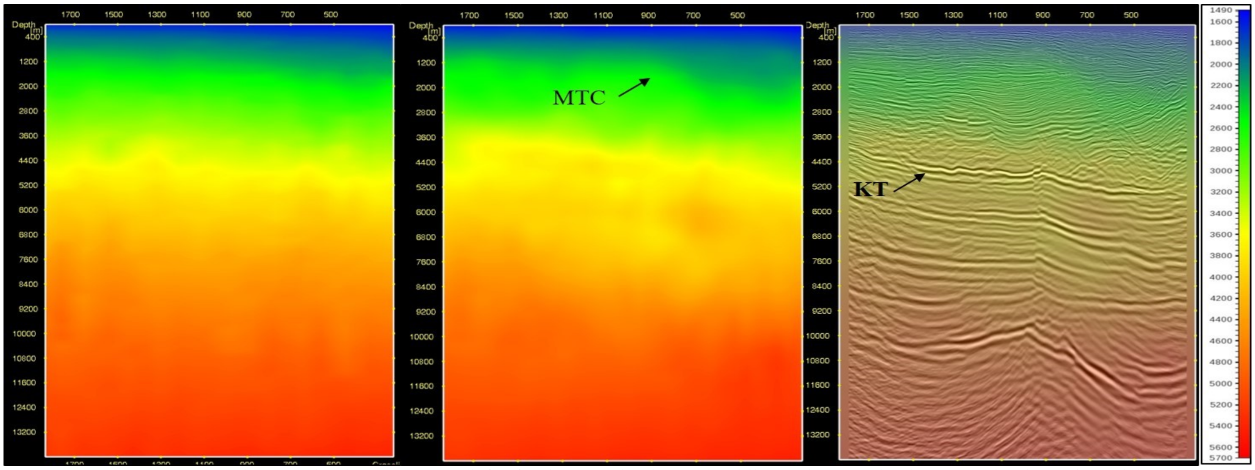

Figure.4 Initial interval velocity section (left), final interval velocity (middle) and interval velocity on depth stack (right)

3D reflection angle-azimuth gathers display reflectivity as a function of opening angle and opening azimuth and are most meaningful in the vicinity of actual local reflecting surfaces. Auto picking seeds point are assigned by Dip-Azimuth-Continuity (DAC) Volume. Full azimuth grid based tomography is performed to update the depth interval velocity. Tomographic matrix is then built that contains a set of coupled equations relating the RMOs with travel time delay along subsurface ray-pair. Finally this tomography matrix is solved in isotropic mode with optimized parameters. The output is updated isotropic depth-interval velocity. Four iterations of tomography is performed at an update cell of 500mx500mx300m (xyz) that gives reasonably flat reflection angle azimuth gathers. Figure.4 shows initial and final interval velocity with the stack section.

Results

In figure.4 velocity increase below KT boundary is observed after tomography. In the final model low velocity zone at the shallower level corresponds to the sediments above MTC and is structurally consistent with MTC boundary. Local angle domain wavefield decomposition is then performed using this final interval velocity. LAD 3D directional angle-azimuth gather decomposed migrated wavefield based on subsurface dip and dip-azimuth at the image point. The direction which have maximum energy is known as specular direction and this direction represents actual reflector dip at that image point. Specular direction mainly contains reflection energy and this energy is termed as specular energy.

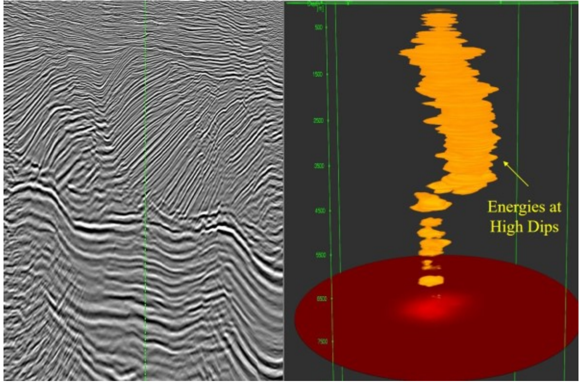

Figure.5 Energy distribution in directional angle-azimuth gather

The remaining energy mostly dominated by diffraction is known as non-specular energy. Figure.5 shows the energy distribution in the directional angle-azimuth gather at the marked cdp location of depth stack. The depth stack has steeply dipping reflectors at the specified cdp location. The same is observed in the directional angle-azimuth gather as the maximum energy holding directions in the gather are at high dips.

Based on the specular direction a specular filter is applied that enhances reflection and on stacking, this energy gives specular stack. The specular stack purely contains enhanced reflection energy. Hence an improvement in the continuity of reflection events in specular stack.

On the other hand a diffraction filter is applied that eliminates specular energy from total wavefield and retains non-specular energy. Stacking of this non-specular energy gives diffraction stack that delineate sub-surface discontinuities.

The section of figure.6 clearly shows enhanced reflector continuity in the specular stack. The growth fault delineation are better than the vintage processed data. Reflectors continuity above the MTC boundary are also enhanced in the specular stack. Continuity enhancement of the deeper reflectors are also seen along with improved fault delineation. High dips reflectors (figure.7) are now imaged with improved fault position. Structural mapping of basement is now possible with good confidence.

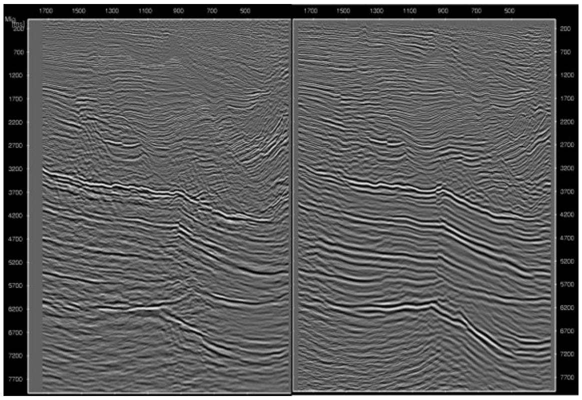

Figure.6 Section comparison on vintage PSTM vs recent specular stack scaled back to time

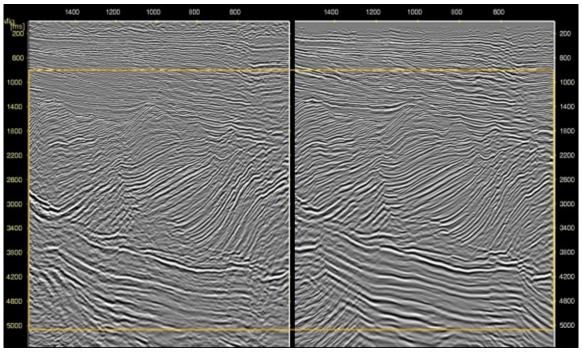

Figure.7 High dips strata imaging, vintage PSTM vs recent specular stack scaled back to time

The diffraction stack on the other hand delineates lateral extent of major-minor faults as seen in figure.9. Discontinuities in the diffraction stack slice not only correlates with the faults in the specular stack but also gives its lateral extent. Diffraction stack also captures energies from very high dips (figure.9). When specular and diffraction stack are combined correlation of these high dips are observed. Combination of this specular and diffraction stack will give good confidence in structural interpretation.

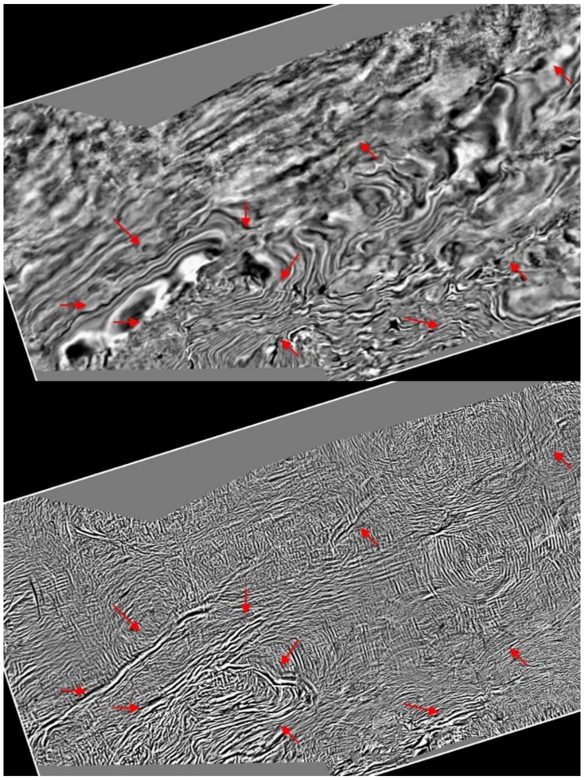

Figure.8 Specular stack slice (top) and diffraction stack slice (bottom) at 2500 ms

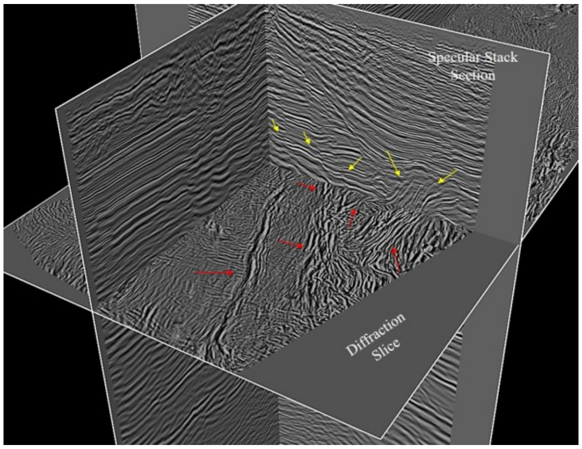

Figure.9 Delineation of faults and high dips using combined specular and diffraction stack

Conclusion

Full azimuth reflection tomography gives a velocity model that gives flat reflection angle azimuth gather. Specular and diffraction imaging successfully separated out reflection and diffraction energy. Enhanced continuity of deep-seated reflector are seen as compared to vintage PSTM data. The fault delineation is also very clear in the specular stack. The diffraction stack properly imaged major-minor faults. Imaging of highly dipping reflector is very clear in diffraction stack. The growth faults are pronounced in specular stack and also agrees with the fault in diffraction stack. Improvement over the earlier processed data in seen in terms of reflector continuity, high-dips imaging and in fault delineations. New outputs will help in identifying hydrocarbon prospect in this area.

References

Zvi Koren and Igor Ravve, 2006, Constrained Dix inversion; GEOPHYSICS, VOL. 71, NO.6 (November-December, 2006); P.R113-R130.

Zvi Koren and Igor Ravve, 2011, Full-azimuth subsurface angle domain wavefield decomposition and imaging Part- I: Directional and reflection image gathers; GEOPHYSICS, VOL. 76, NO.1 (January-February, 2011); P.S1-S13.

Igor Ravve and Zvi Koren, 2011, Full-azimuth subsurface angle domain wavefield decomposition and imaging: Part 2 — Local angle domain; GEOPHYSICS, VOL. 76, NO.2 (March-April, 2011); P.S51-S64.

Acknowledgments

The authors are thankful to Director (Exploration), Oil and Natural Gas Corporation Limited for providing the opportunity to carry out this project. The authors are also thankful to HOI-GEOPIC and Head Processing Division, GEOPIC for their valuable suggestions. The authors would like to thank ONGC for giving permission to publish the work.

Views expressed in this paper are those of the authors only and does not refer to any views of ONGC.